Cycloaddition between nitrogen-doped graphene (6π-componpleent) and benzene (4π-component): a theoretical approach using density functional theory with vdW-DF correction.

E. Rangel-Cortes, J.A. Pescador-Rojas, V.A. Cardozo-Mata, A. Hernández-Hernández, E. Vallejo-Castañeda, L.A. Hernández-Hernández, T. Romero-Cortes

Supplementary Information

Theoretical Method

The formation energy of vacancies in graphene and in N-doped graphene were calculated according to the next relations

$$\Delta E_f = E_{(GN_xV_y)} + (x + y)\mu_C - (E_G + x\mu_N)$$

$$\Delta E_f = E_{(G_{x+y})} + (x + y)\mu_C - (E_G)$$

In this context, $NxVy$ represents the defect. x is the number of carbon atoms substituted by N nitrogen atoms, and y is the number of V vacancies. $x + y$ is the total carbon atoms removed from the perfect graphene (G) sheet to form the defects. μ_C is the perfect graphene per atom total energy, μ_N is a half of the total energy of the N_2 molecule in the gas phase, E_G is the perfect (pristine) graphene energy and $E_{(GN_xV_y)}$ is the N-doped G-graphene with y-vacancy system energy (see reference 27).

Table 1S

The adsorption distance of the benzene molecule (C_6H_6) on nitrogen-doped graphene defects. The exchange–correlation functional of Perdew-Burke-Ernzerhof (PBE) was applied.

PBE				
N_3V_1 pyridinic - C_6H_6		Coordinates		Distance (Å)
	x	y	z	
N	2.482568924	7.135273970	-0.740295771	**5.70901172**
C	1.668169796	4.097897966	4.024566857	
N_3V_1 pyrrolic - C_6H_6		Coordinates		Distance (Å)
	x	y	z	
N	1.310076511	3.447027430	-0.863887813	**4.96353213**
C	1.175998118	4.211987201	4.038510654	
N_3V_3 pyrrolic - C_6H_6		Coordinates		Distance (Å)
	x	y	z	
N	9.040811435	-0.325903785	0.432283738	**1.55360526**
C	9.199480542	-0.636451133	1.946243372	
N_4V_2 pyridinic - C_6H_6		Coordinates		Distance (Å)
	x	y	z	
N	1.160658653	5.009403825	-0.265870361	**4.24337605**
C	1.938619962	5.272982905	3.897246566	

Table 2S

The adsorption distance of the benzene molecule (C_6H_6) on nitrogen-doped graphene defects. The exchange–correlation functional of Perdew-Burke-Ernzerhof (PBE) was applied and dispersion corrections were included by employing the vdW-DF approach, as proposed by the Thonhauser group.
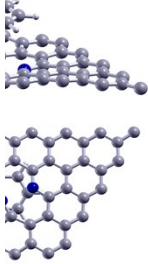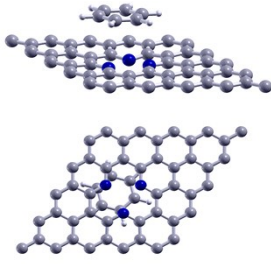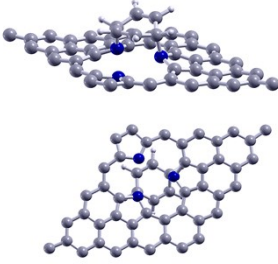
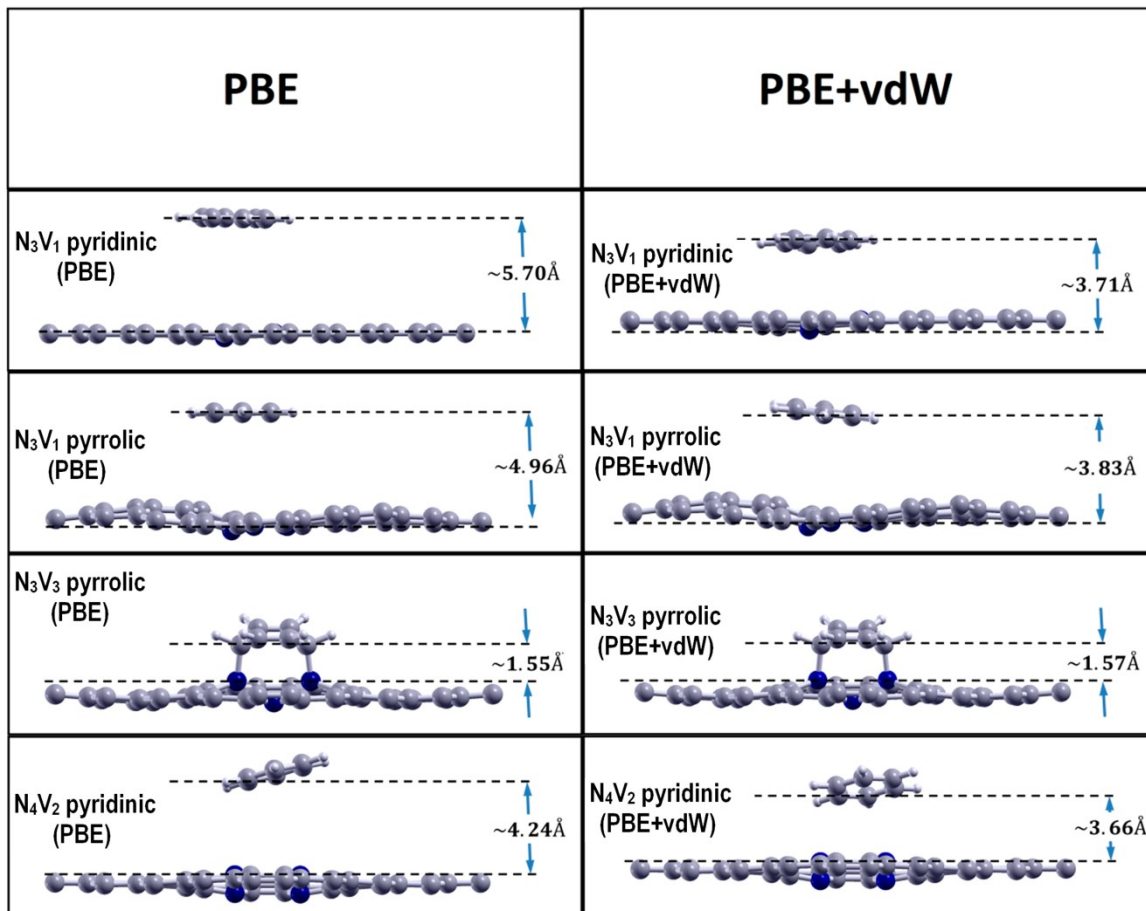|	**PBE+vdW**			
N_3V_1 pyridinic - C_6H_6		Coordinates		Distance (Å)
	x	y	z	
N	1.215889662	4.906187928	-0.469538084	**3.71117575**
C	0.612024514	5.149598725	3.184079782	
N_3V_1 pyrrolic - C_6H_6		Coordinates		Distance (Å)
	x	y	z	
N	3.760678856	4.898464952	-0.708378584	**3.83273389**
C	2.677823838	4.075838941	2.874994200	
N_3V_3 pyrrolic - C_6H_6		Coordinates		Distance (Å)
	x	y	z	
N	9.058131304	-0.333578335	0.420600162	**1.5781897**
C	9.197787815	-0.638090137	1.962823018	
N_4V_2 pyridinic - C_6H_6		Coordinates		Distance (Å)
	x	y	z	
N	1.114030849	5.001821188	-0.050626490	**3.66909799**
C	2.859063388	6.495116745	2.810703593	

Table 1S and Table 2S compare the adsorption distance between benzene and nitrogen-doped graphene defects (N_3V_1 and N_4V_2 pyridinic, N_3V_3 and N_3V_1 pyrrolic) with both methods. In Fig. 1S, is shown the configurations between benzene and nitrogen-doped graphene defects with PBE method. Thus, these results show that benzene is physisorbed onto N_3V_1 pyrrolic and N_3V_1 and N_4V_2 pyridinic. The adsorption distance computed with PBE increases about 16~54 % compared to those with PBE+vdW, except for the N_3V_3 pyrrolic defect system. On the other hand, PBE method is accurate enough to reproduce the electronic properties of chemisorbed species. However, it cannot describe the physisorption regime because the non-local correlation effects needed to address the dispersion interactions are not included. For interaction between N_3V_3 pyrrolic and

benzene, the errors associated with DFT formalism at large distances and associated with dispersion interactions are smaller than those involved in making or breaking chemical bonds.

Table 3S

The adsorption distance and energy adsorption of the benzene molecule (C_6H_6) on nitrogen-doped graphene defects, as well as the average length between neighboring N atoms. The exchange–correlation functional of Perdew-Burke-Ernzerhof (PBE) was applied with dispersion corrections by employing the vdW-DF approach.

yridinic	N_3V_1 pyrrolic	N_3V_3 pyrrolic
	PBE+vdW	
.71	3.83	1.58
4.57	54.813	242.18
50 meV)	(568.10 meV)	(2.51 eV)
.55	2.55	3.09

Fig. 1S. The adsorption of the benzene molecule (C_6H_6) on NG defects. Benzene adsorbed onto N_3V_1 pyridinic, N_3V_1 pyrrolic, N_3V_3 pyrrolic, and N_4V_2 pyridinic defects.
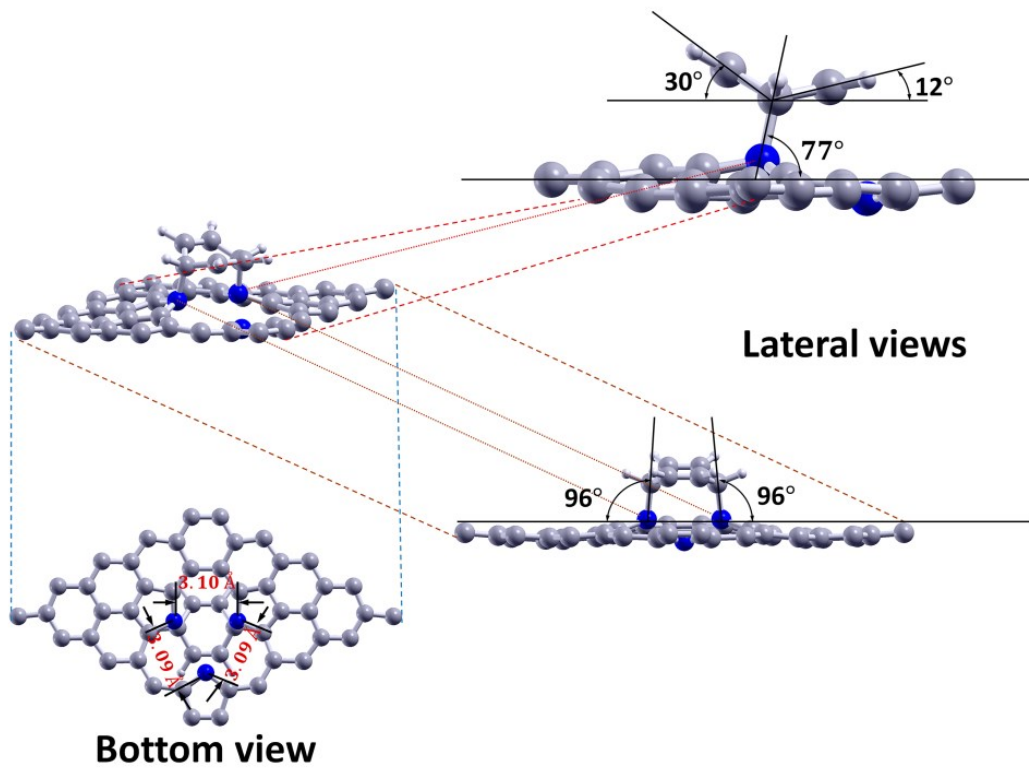
Fig. 2S. Cycloadduct geometry: angles and distances for the benzene adsorption on N_3V_3 pyrrolic defect.

The [6+4] cycloaddition reaction can be statistically modeled using the Arrhenius law.

$$\nu = \nu_0 exp\left[\frac{-\Delta E}{k_B T}\right]$$

Here, the ν rate at a given temperature T is determined using the barrier energy ΔE (see Fig. 2) and the attempt frequency ν_0 (k_B is the Boltzmann constant). In the following, temperature T and an attempted frequency ν_0 will be used to model our systems. The ν_0 value is motivated by the estimate of the phonon frequency of $\nu_0 = k_B T/h \approx 10^{12}$ Hz (h, is the Planck's constant). Assuming ν maximum (0.10 s^{-1}) and minimum (1×10^{-6} s^{-1}). Then, reaction barrier energies as a function of temperature can be observed in Fig. 3S, while Fig. 4S shows isotherms and frequencies as a function of reaction barrier energy, maximum hopping frequency (0.1 s^{-1}). Our results suggest that the reactions occur in the range of hours at temperatures about of 500 K. This temperature it's enough for activated the cycloaddition with high endothermic reaction about 96.485 kJ/mol (1.0 eV).

On the other hand, the product's energies are shown to be higher than those of the reactant. Therefore, processes are endothermic reactions with a positive change in enthalpy ($\Delta H > 0$) and an increase in entropy ($\Delta S > 0$). For this reason, the most probable reaction pathway is the cycloaddition in temperature about 500 K. Thus, if we have enough energy, Gibbs free energy can become negative so that the reaction will go smoothly and efficiently. Thus, the cycloreversion of the Gibbs free energy is positive and could not occur.
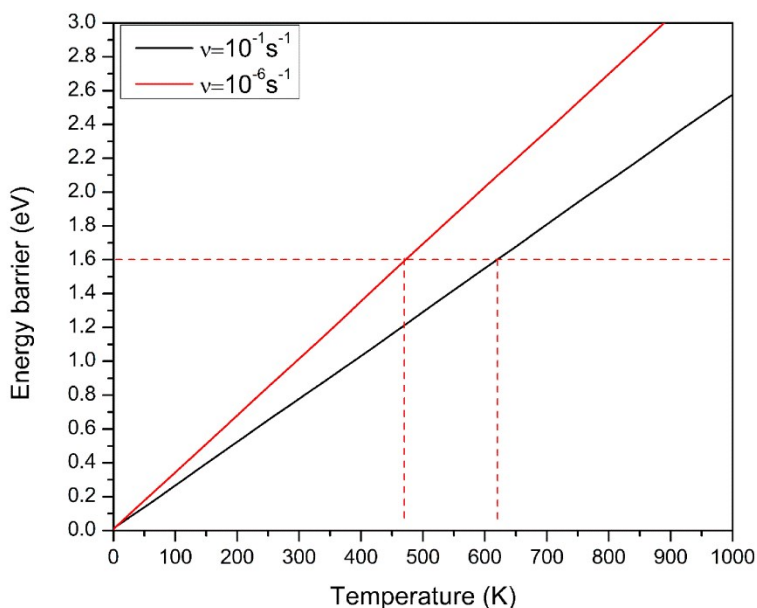

Fig. 3S. According to the Arrhenius law, reaction energy barriers as a function of temperature for two observable hopping frequencies of 0.1 s^{-1} (maximum) and 1×10^{-6} (minimum) are given.
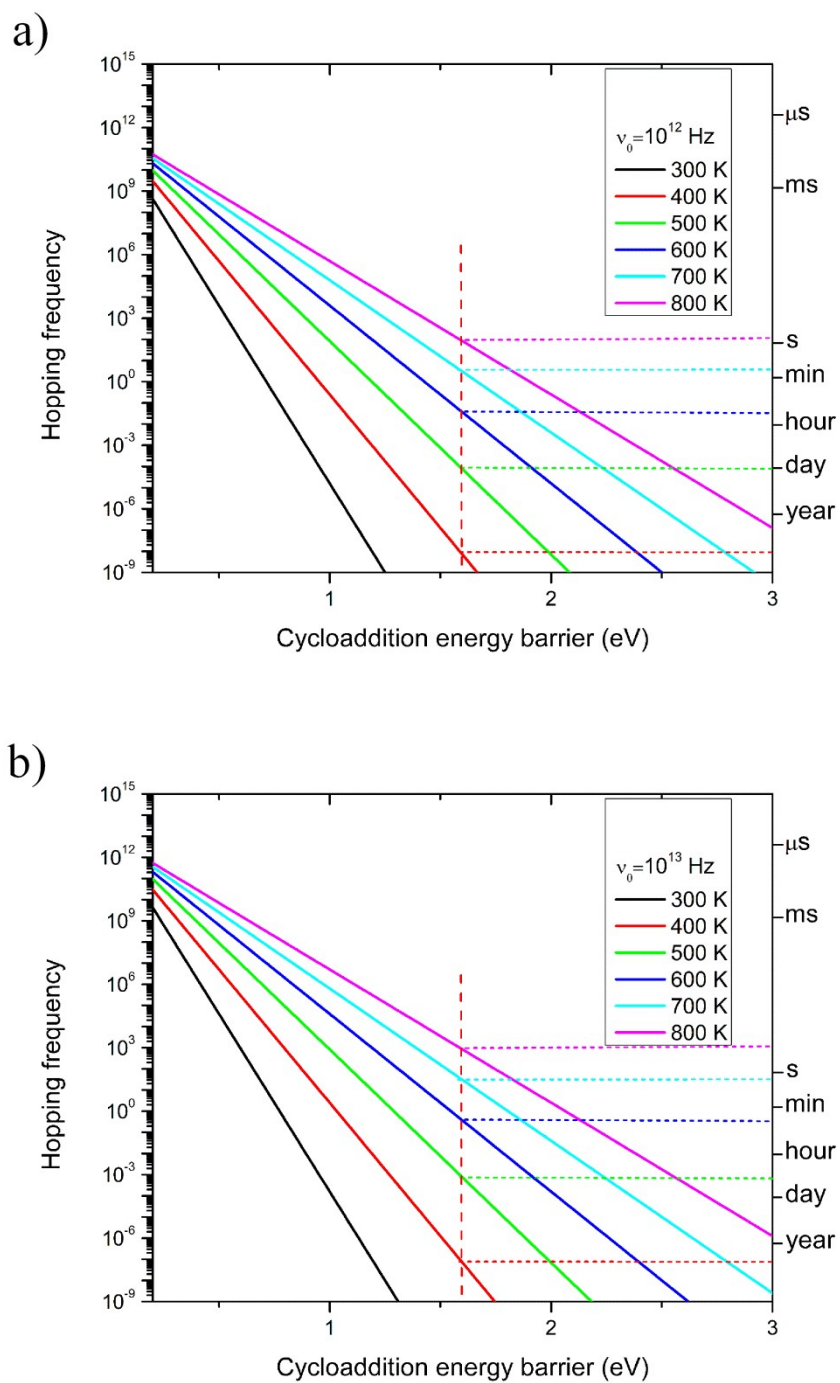
Fig. 4S. The frequency for different reaction energy barriers (normalized to 1000) in dependence of the temperature for **a)** $\nu_0 = 10^{12}$ Hz and **b)** $\nu_0 = 10^{13}$ Hz. The observable hopping frequencies of 0.1 s^{-1} (maximum) was considered.
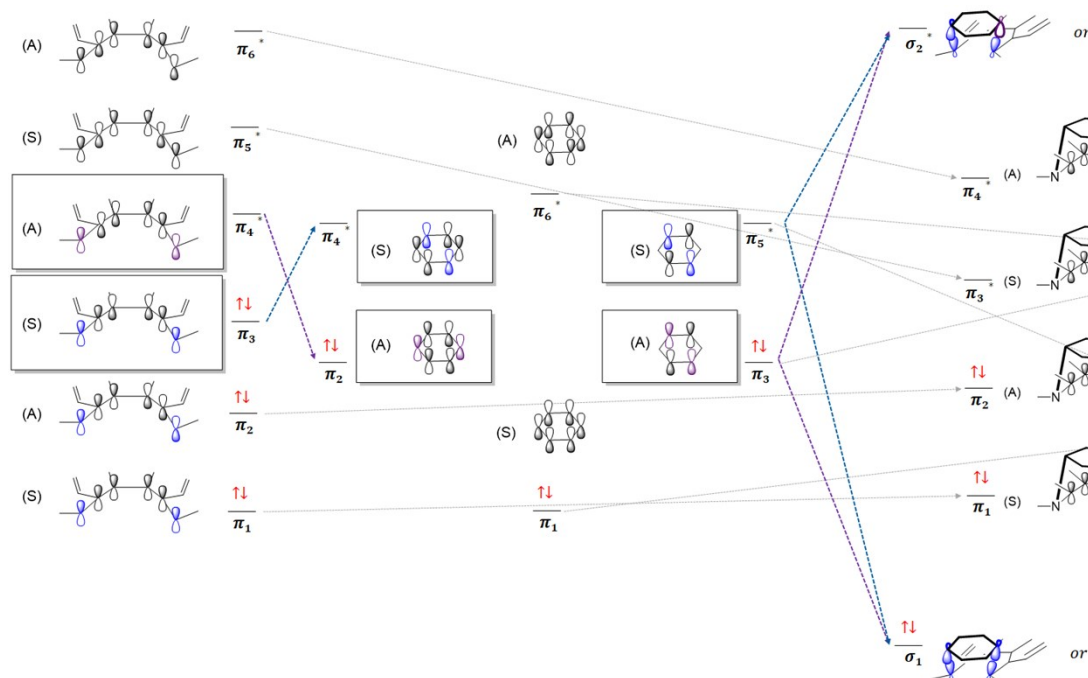
Fig. 5S. Orbital correlation diagram (specular symmetry). The constructive combination between **HOMO (GN) - LUMO (benzene)** or **LUMO (GN) – HOMO (benzene)** orbitals produces a bonding orbital σ_1 and another anti-bonding σ_2^*, during cycloaddition the nitrogen atoms are rehybridized from sp^2 to sp^3, which produces orbitals sets splitting corresponding to diene ($\pi_1 - \pi_4^*$) and two double bonds ($\pi_{1'} - \pi_{2''}^*$ and $\pi_{1''} - \pi_{2'}^*$). Relative position of orbitals is arbitrary and does not reflect relative energy of different orbitals involved in [6 + 4] cycloaddition, based on considerations of orbital specular symmetry of reacting pi systems proposed by Woodward–Hoffmann.

Optimization of the Nitrogen-doped Graphene (NG) system, with pyridinic (N_3V_1, N_4V_2) and pyrrolic (N_3V_1, N_3V_3) defects, deposited on Cu (1 1 1) substrate (see Fig. 1 in reference 46). The NG can be placed on the Cu (1 1 1) substrate with each N atom superimposed on a single Cu atom. Furthermore, the Cu slab was modeled and optimized into three layers, each composed of 25 atoms. The chemical interaction (binding energy) between three, four, and five copper layers with NG defects were similar, suggesting that three layers are sufficient. To investigate the interactions of NG on the Cu (1 1 1) surface, a Cu super-cell was employed, conforming three atomic (5×5) Cu layers stacked in the z direction.
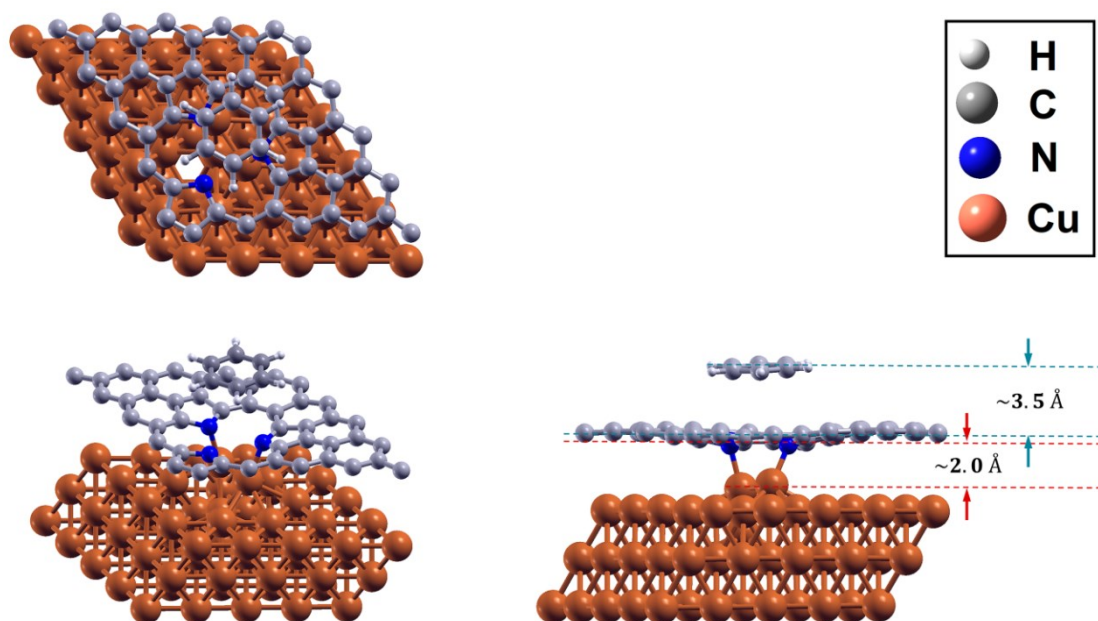
Fig. 6S. Adsorption of the benzene molecule (C_6H_6) on NG/Cu (1 1 1). Benzene adsorbed onto N_3V_3 pyrrolic defect deposited on 5×5×3 Cu (1 1 1) substrate